etadata, citation and similar papers at core.ac.uk

Accepted Manuscript

Title: Cognitive deficits induced by multi-walled carbon nanotubes via the autophagic pathway

Author: Jing Gao Xiaochen Zhang Mei Yu Guogang Ren Zhuo Yang

PII: S0300-483X(15)30031-7
DOI: http://dx.doi.org/doi:10.1016/j.tox.2015.08.011
Reference: TOX 51586

To appear in: *Toxicology*

Received date: 15-6-2015
Revised date: 26-8-2015
Accepted date: 26-8-2015

Please cite this article as: Gao, Jing, Zhang, Xiaochen, Yu, Mei, Ren, Guogang, Yang, Zhuo, Cognitive deficits induced by multi-walled carbon nanotubes via the autophagic pathway.Toxicology http://dx.doi.org/10.1016/j.tox.2015.08.011

This is a PDF file of an unedited manuscript that has been accepted for publication. As a service to our customers we are providing this early version of the manuscript. The manuscript will undergo copyediting, typesetting, and review of the resulting proof before it is published in its final form. Please note that during the production process errors may be discovered which could affect the content, and all legal disclaimers that apply to the journal pertain.

ACCEPTED MANUSCRIPT

Cognitive deficits induced by multi-walled carbon nanotubes via the autophagic pathway

Jing Gao [1], Xiaochen Zhang [1], Mei Yu [2], Guogang Ren [3], Zhuo Yang[1]*

[1]College of Medicine, State Key Laboratory of Medicinal Chemical Biology, Tianjin Key Laboratory of Tumor Microenvironment and Neurovascular Regulation, Nankai University, Tianjin 300071, China; [2]College of Life Science, Nankai University, Tianjin 300071, China; [3]Science and Technology Research Institute, University of Hertfordshire, Hatfield, Herts AL10 9AB, UK

Correspondence for Proofs:

Professor YANG Zhuo, College of Medicine, Nankai University,

Tianjin 300071, China

Tel: 86-22-23504364

Fax: 86-22-23502554

Email: zhuoyang@nankai.edu.cn

ACCEPTED MANUSCRIPT

Graphical abstract

Abstract: Multi-walled carbon nanotubes (MWCNTs) have shown potential applications in many fields, especially in the field of biomedicine. Several studies have reported that MWCNTs induce apoptosis and oxidative damage in nerve cells during *in vitro* experiments. However, there are few studies focused on the neurotoxicity of MWCNTs used *in vivo*. Many studies have reported that autophagy, a cellular stress response to degrade damaged cell components, can be activated by diverse nanoparticles. In this study, we investigated the neurotoxic effects of MWCNTs on hippocampal synaptic plasticity and spatial cognition in rats. Then, we used an inhibitor of autophagy called chloroquine (CQ) to examine whether autophagy plays an important role in hippocampal synaptic plasticity, since this was damaged by MWCNTs. In this study, adult male Wister rats were randomly divided into three groups: a control group, a group treated with MWCNTs (2.5mg/kg/day) and a group treated with MWCNTs+CQ (20mg/kg/day). After two-weeks of intraperitoneal (i.p.) injections, rats were subjected to the Morris water maze (MWM) test, and the long-term potentiation (LTP) and other biochemical parameters were determined. Results showed that MWCNTs could induce cognitive deficits, histopathological alteration and changes of autophagy level (increased the ratio of LC3 II /LC3 I and the expression of Beclin-1). Furthermore, we found that CQ could suppress MWCNTs-induced autophagic flux and partly rescue the synapse deficits, which occurred with the down-regulation of NR2B (a subunit of NMDA receptor) and

ACCEPTED MANUSCRIPT

synaptophysin (SYP) in the hippocampus. Our results suggest that MWCNTs could induce cognitive deficits *in vivo* via the increased autophagic levels, and provide a potential strategy to avoid the adverse effects of MWCNTs.

Keywords: MWCNTs; Cognitive deficits; Autophagy; Chloroquine; Rats

ACCEPTED MANUSCRIPT

1 Introduction

Nanomaterials have shown increasing usage worldwide since their emergence a few decades ago. Carbon nanotubes (CNTs) are one of the best known nanomaterials due to their unique chemical and physical characteristics (Nakashima and Fujigaya, 2007; Wang et al., 2007). CNTs have shown increasing promise in the field of biomedicine in recent years. CNTs, especially multi-walled carbon nanotubes (MWCNTs), have many applications in medical neuroscience, including as drug carriers (Bianco et al., 2005; Yang et al., 2009), in electrical nerve stimulation (Keefer et al., 2008), and as substrates for nerve cell growth and differentiation (Chao et al., 2009; Chao et al., 2010; Sorkin et al., 2006). Moreover, CNTs have been used to deliver drugs and genetic material into nerve cells in the brain for the treatment of glioma and neurodegenerative diseases because of their ability to pass through cell membranes (Ren et al., 2012; Yang et al., 2010b). Because they have such widespread applications, it is necessary to explore the potential risks that CNTs might pose to human health. A number of studies performed with CNTs have evaluated their toxicity to different organs, such as the lungs, kidneys, and liver (Awasthi et al., 2013; Deng et al., 2009; Li et al., 2007). Several *in vitro* studies have confirmed that CNTs could generate neurotoxic effects, including decreasing cell activity (Belyanskaya et al., 2009; Zhang et al., 2010). In addition, our previous studies have showed that MWCNTs induce cytotoxicity in C6 cells (Han et al., 2012) and inhibit CA1 glutamatergic synaptic transmission in rat hippocampal slices *in vitro* (Chen et al., 2014). However, there is no accurate conclusion about the impaction of CNTs on the nervous system *in vivo*.

Autophagy, which is a highly conserved lysosomal degradation pathway, plays an important role in maintaining cytoplasmichomeostasis (Das et al., 2012; Mizushima

ACCEPTED MANUSCRIPT

and Komatsu, 2011). It is a dynamic physiological process that is necessary for cellular health and survival (Kroemer et al., 2010). Damaged and aging cells or organelles are degraded by autophagy. The double membraned autophagosomes, which can deliver cytosolic components to the lysosome for degradation and recycling, are formed following the activation of the autophagic pathway (Mizushima, 2007). The inactive cytoplasmic LC3 (LC3 I), which is a soluble protein distributed ubiquitously in mammalian tissues and cultured cells, can be converted into the active membranous LC3 II, which triggers the formation of the autophagic vesicle (Mizushima et al., 2010). Thus the ratio of LC3 II/LC3 I is widely used to estimate the level of autophagy. Furthermore, another autophagy-related (Atg) gene Beclin 1 is necessary for the localization of autophagic proteins to a pre-autophagosomal structure. Overexpression of Beclin-1 can improve the level of autophagy activity by interacting with the class III type phosphoinositide 3-kinase (PI3KC3)/Vps34 (Kang et al., 2011). It is well known that autophagy protects cells against accidental death (Kaushik et al., 2011). Indeed, many studies have shown that physiological autophagy is responsible for the survival of neurons (Poels et al., 2012). Cell death that displays the typical features of autophagy such as a massive cytoplasmic vacuolization is defined as “autophagic cell death”(Shen et al., 2012). Recently, some nanoparticles have been regarded as autophagy activators, such as gold nanoparticles (Ma et al., 2011) and TiO_2 nanoparticles (Kenzaoui et al., 2012). Also, reports have indicated that disordered autophagy could disrupt the flow of pre-synaptic terminals and cause axonal dystrophy (Sanchez-Varo et al., 2012). However few reports have illuminated

ACCEPTED MANUSCRIPT

the relationship between synaptic plasticity and the autophagy of neurons caused by MWCNTs.

In this study, behavioral changes, electrophysiological tests and biochemical indexes were used to determine changes of synaptic plasticity after exposure to MWCNTs. We investigated whether MWCNTs could contribute to autophagy enhancement and synaptic plasticity impairment in the CA1 area *in vivo*, and we explored the relationship between autophagic flux and the synaptic plasticity damage caused by MWCNTs. We proved that CQ could prevent MWCNTs-induced synaptic impairment by down-regulating autophagy. These results may reveal a key mechanism of autophagy in the nervous system under MWCNTs treatment, and give experimental basis for the safety of biomedical applications of MWCNTs. Our observation may provide a new potential therapeutic method to relieve synaptic impairment induced by MWCNTs.

2 Materials and methods

2.1 Materials and reagents

The MWCNTs used in this study were obtained from the Institute of Metal Research, China Academy. The average length of MWCNTs was approximately 2μm and the diameter was approximately 10–20nm. The MWCNTs were suspended in 0.9% NaCl with 0.1% Tween 80, and the suspensions were sonicated for 20 minutes before each use. The characteristics of the nanoparticles used in this study can be found in our previous study (Han et al., 2012).

ACCEPTED MANUSCRIPT

Anti-NMDAR2B antibody and anti-Synaptophysin antibody were purchased from Abcam (Cambridge, UK). Anti-LC3 antibody was obtained from MBL (Nagoya, Japan). Anti-Beclin-1 antibody was purchased from Cell Signaling Technology (MA, USA). Anti-β-actin antibody was purchased from Santa Cruz Biotechnology, Inc. CA (California, USA).

2.2 Animals and treatment

Specific-pathogen free (SPF) adult male Wistar rats, weighing 200–220 g, were purchased from the Experimental Animal Center of the Chinese Academy of Medical Science, and reared in the Animal House of Medical School in Nankai University. Conditions were kept at 22±2°C, and rats were housed in pairs in clear plastic cages on a 12:12 h light/dark cycle with *ad libitum* access to food and water. All experiments were performed according to protocols approved by the Committee for Animal Care at Nankai University and in accordance with the practices outlined in the NIH Guide for the Care and Use of Laboratory Animals. Rats were acclimated for one week before exposure.

Animals were randomly divided into three groups, a control group (n = 8), a MWCNTs-treated group (n = 8) and a MWCNTs+CQ group (n = 8). In the MWCNT group, rats were treated with MWCNTs at a dose of 2.5mg/kg (Muller et al., 2005) via intraperitoneal (i.p.) injection once per day over 14 consecutive days. Rats in the MWCNTs+CQ group were i.p. injected with CQ (20mg/kg/d, Wako Pure Chemical Industries, Ltd., Osaka, Japan) (Maeda et al., 2013) dissolved in a suspension, 30

ACCEPTED MANUSCRIPT

minutes before the MWCNTs injection, while the animals in the control group received the same dose of only the suspension without CQ.

2.3 Physical observation

Each rat was weighed and recorded every two days at the same time over the 14 days.

2.4 Morris water maze test

After 14 days of treatment, all rats of every group were trained and tested with the Morris water maze (MWM, RB-100A type, Beijing, China) to monitor their spatial learning and memory behaviors. This system involves a circular tub (height 60cm, diameter 150cm) and a device, which is connected to a personal computer to capture the rat's swimming pathway. The maze was filled with water maintained at 25±1°C and dyed by nontoxic black ink. The water was divided into four equal quadrants (I–IV), and a 10-cm-diameter platform, whose surface was 1.5-2 cm below the water surface, was positioned in the middle of quadrant III.

The test consisted of two consecutive stages, initial training and re-acquisition training. Each stage included two phases called the place navigation phase and the spatial probe phase. During the navigation phase, rats were subjected to two sessions (each session consisted of four trials) of training per day for five consecutive days. In each trial, the animals were gently put into the water from a random point of the quadrant. The rats were given 60s to learn to find the hidden platform. During this stage, the time it took for rats to find the platform (escape latency) and the swimming

ACCEPTED MANUSCRIPT

speed were recorded. If a rat failed to locate the platform within 60s, it was guided by the experimenter to stay on the platform for 10s, and its escape latency was recorded as 60s. The interval between each of the trials was approximately 10 minutes. The order of starting points was the same for all animals. The rats were given the spatial probe trial test 24h after the last trial of the navigation phase. The platform was removed during the spatial probe phase. Rats were released individually into water from the starting point of quadrant I and allowed to swim freely for 60s. Only one trial was carried out in this phase. Quadrant dwell time (the percentage of time spent in the target quadrant) and platform crossings (numbers of times the rat passed the platform area) were measured. After that, re-acquisition training was performed immediately to examine the learning flexibility. The methods used and parameters recorded were the same as those in place navigation phase and spatial probe phase except the platform was moved to the contra lateral quadrant.

2.5 *In vivo* electrophysiological testing

The LTP and depotentiation were measured after rats had undergone the MWM test. The protocols used were similar to those described in our previous study (An et al., 2013; Han et al., 2014). Rats were positioned on a stereotaxic frame (SR-6 N; Narishige, Japan) for surgery and observed after being anesthetized with 30% urethane (0.4 ml/kg, i.p.). Surgery was performed on the left side of brain. A proper incision was cut in the scalp and a small hole was drilled in the skull for both recording and stimulating electrodes. In stereotaxic coordinates, a bipolar stimulating

ACCEPTED MANUSCRIPT

electrode was implanted in hippocampal Schaffer collaterals (4.2 mm posterior to bregma, 3.5 mm left to midline, 2.3-2.6 mm ventral below the dura), and the recording electrode was positioned in the stratum radiatum area of hippocampal CA1 (3.5 mm posterior to bregma, 2.5 mm left to midline, 2.0–2.2 mm ventral below the dura). Test stimuli were transmitted to Schaffer collaterals every 30 s at an intensity (range 0.3–0.5mA) that could evoke a response of 70% of its maximum. Subsequently, sampling was made under single-pulse stimulation (stimulus pulse with 0.2 ms at 0.05 Hz) for 30 minutes as the base line. After that, a theta burst stimulation (TBS, 30 trains of 12 pulses at 200 Hz) was delivered to induce LTP. The single-pulse recording was done every 60 s for 60 minutes following TBS. Afterwards, low-frequency stimulation (LFS, 900 pulses of 1 Hz for 15 minutes) was delivered to induce depotentiation. Then, single-pulse recording was resumed every 60 seconds for 60 minutes. All initial measurements were executed in a Clampfit 10.0 (Molecular Devices, Sunnyvale, CA). After the electrophysiological experiment, rats were sacrificed and brains were removed for hematoxylin and eosin staining and a Western blot assay.

2.6 Western blot analysis

The hippocampus was removed and promptly stored at -80°C until needed. Firstly, every hippocampus was grinded and lysed in 200 μl lysis buffer (Beyotime Biotechnology, Haimen, China), which contained Phenylmethanesulfonyl fluoride (PMSF,1:100 dilutions). Next, the lysates were centrifuged at 12000rpm for 20–30 minutes at 4°C. The supernatant was mixed with loading buffer (4:1 ratio) and boiled

ACCEPTED MANUSCRIPT

in boiling water for 20 minutes. Whole proteins were electrophoresed in a 10–13% SDS-PAGE gel and then transferred to polyvinylidene fluoride (PVDF) membranes (0.45μm). After that, the PVDF membranes were incubated with 5% skim milk, then incubated with primary antibody overnight at 4°C. The PVDF membranes were incubated with secondary antibody after washing thrice with TBST. Protein band intensities were detected with a chemiluminescence detection kit (Pierce) and exposed to X-ray film (Eastman Kodak, Rochester, NY). Equal protein loading was ensured by using β-actin expression using a mouse monoclonal antibody (1:1000 Santa Cruz).

2.7 Hematoxylin/eosin staining

When brains were isolated from the sacrificed rats, they were perfused with 0.1 mol/l phosphate buffer (pH 7.4) immediately. Next the brains were removed and immersed in 4% paraformaldehyde and fixed at 4°C for at least 24h. After that, they were dehydrated through a graded sucrose solution and embedded in OCT compound (Tissue-Tek, Miles) for tissue sectioning. The coronary slices (10 mm) stained with hematoxylin/eosin (HE) were photographed on a Leica microscope (Wetzlar, Germany).

2.8 Data and statistical analysis

All data were presented as mean ± S.E.M. Data. Differences in performance of spatial probe phase, electrophysiological recordings and Western blot assays were evaluated using a one-way ANOVA. A two-way repeated measure ANOVA was employed to analyze the differences in place navigation phase and the body weight over time in each rat. All analyses were performed using SPSS (17.0) software and differences

ACCEPTED MANUSCRIPT

were considered significant when $P<0.05$.

3 Results

3.1 Body weight

As shown in Fig. 1, the body weight in all groups increased during the 14 days. The mean rat weight in the MWCNTs group was almost as heavy as that of the Contol group (Fig. 1, $P>0.05$). There were no differences in body weights between MWCNTs-treated group and MWCNTs+CQ group (Fig. 1, $P>0.05$).

3.2 Initial training of MWM experiment

The cognitive ability of all groups is shown in Fig. 2. The escape latencies of all rats decreased gradually throughout 5 days of training (Fig. 2A). Two-way repeated measures ANOVA showed that the mean escape latency statistically increased in the MWCNTs group from day 2 to day 5 compared to that of the Control group (Fig. 2A, day 2 to day 5, $P<0.05$). There was a significant decrease in mean escape latency in the MWCNTs +CQ group compared to that of the MWCNTs group (Fig. 2A, $P<0.05$). There were no significant differences in swimming speeds between the three groups (Fig. 2B, $P>0.05$). The spatial probe test was carried out on the sixth day. Results showed that both mean number of platform crossings (Fig. 2C, $P<0.001$) and mean quadrant dwell time (Fig. 2D, $P<0.001$) were significantly decreased in the MWCNTs group compared to the Control group. In the group treated with CQ, the mean number of platform crossings (Fig. 2C, $P <0.05$) and the mean quadrant dwell time (Fig. 2D, $P<0.05$) were significantly elevated.

3.3 Re-acquisition training of MWM test

During the re-acquisition training stage, the escape latencies were reduced in all

ACCEPTED MANUSCRIPT

groups. For the MWCNTs treatment group, the mean escape latency was significantly longer compared to those in the Control group (Fig. 3A, $P<0.001$ for day 2 and day 3). Furthermore, the mean escape latency was reduced in the MWCNTs+CQ group compared to those in the MWCNTs group (Fig. 3A, $P<0.05$). In addition, there were no differences in swimming speeds between the three groups (Fig. 3B, $P>0.05$). The mean number of platform crossings (Fig. 3C, $P<0.01$) and the mean quadrant dwell time (Fig. 3D, $P<0.01$) were significantly decreased in the MWCNTs group compared to the Control group. The above parameters were increased (Fig. 3D, $P<0.05$) in the MWCNTs+CQ group compared to the MWCNTs group.

3.4 LTP and depotentiations from Schaffer collaterals to CA1

As shown in Fig. 4A, the fEPSPs baseline before TBS was quite stable during 30 minutes of low-frequency test stimulations. After TBS stimulation, the fEPSPs slopes were considerably increased in the following 1 hour. Moreover, it was found that fEPSPs slopes were significantly lower in the MWCNTs group compared to those in the Control group (Fig. 4B, $P<0.001$). The fEPSPs slopes in the MWCNTs+CQ group were dramatically increased compared to those in the MWCNTs group (Fig. 4B, $P<0.001$).

To examine whether MWCNTs affected depotentiation, a LFS induction protocol was used for eliciting significant depotentiation (Fig. 4C). LTP-evoked responses of the last 30 minutes were normalized and used as the baseline of depotentiation (1 per minute, Fig. 4C). As shown in Fig. 4D, there was a significant difference in fEPSP slopes between the MWCNTs group and the Control group ($P<0.001$), while fEPSPs slopes were reduced in the MWCNTs+CQ group compared to those of the MWCNTs group ($P< 0.001$).

ACCEPTED MANUSCRIPT

3.5 Western blot analysis

Two types of proteins that are related to synaptic plasticity, called NR2B (180 kDa) and SYP (38 kDa), were detected using Western blot assay. It was shown that NR2B and SYP expressions were decreased in hippocampus of rats in the MWCNTs group compared to those in the Control group (Fig. 5A), and there was a statistically significant difference in NR2B expression between the two groups (Fig. 5B, $P<0.001$). Decreased expression of SYP was also observed (Fig. 5C, $P<0.001$). NR2B (Fig. 5B, $P<0.01$) and SYP (Fig. 5C, $P<0.01$) expression levels were increased dramatically in the MWCNTs+CQ group compared to those of MWCNTs group.

The LC3 II to LC3 I ratio and Beclin-1 levels were measured to assess the level of autophagy. LC3 I is cleaved to LC3 II during the process of autophagy, so the LC3 II/LC3 I ratio is increased when the level of autophagy is elevated (Klionsky et al., 2007). As shown in Fig. 5E , the ratio of LC3 II/LC3 I was significantly increased in the MWCNTs-treated group compared to the Control group ($P<0.001$), and a similar result in the Beclin-1 level was observed from this study (Fig. 5F, $P<0.001$). Statistically significant differences in the LC3 II/LC3 I ratios (Fig. 5E, $P<0.001$) and Beclin-1 levels (Fig. 5F, $P<0.05$) in the MWCNTs+CQ group compared to the MWCNTs group were found.

3.6 Histopathological observation

From the aforementioned results, it is evident that MWCNTs produced degenerative changes in rats. Furthermore, histological analysis was used to observe the neuropathological alterations of CA1 neurons in each group. As seen in Fig.6A, pyramidal cells exhibited regular and compact arrangement in the hippocampal CA1

ACCEPTED MANUSCRIPT

region in the Control group; the neurons were full and the nuclei were light-stained. In contrast, there appeared to be morphological changes in the arrangement of pyramidal cells in the MWCNTs group. The cells became loose and disordered, and showed shortening and deformations in cell shape (Fig. 6B). The injuries were improved in the MWCNTs+ CQ group compared to the MWCNTs group (Fig. 6C).

4 Discussion

Carbon nanotubes are one of the most applicable nanomaterials due to their unique chemical and physical characteristics (Nakashima and Fujigaya, 2007; Wang et al., 2007). They have been used as a brain-targeting vector to delivery drugs and therapy (Yang et al., 2010a). Researchers reported that the viability of cells in the CNS could be reduced after treatment with MWCNTs (Han et al., 2012). One of our previous studies found that the glutamatergic synaptic transmission of CA1 was inhibited in rat hippocampal slices by MWCNTs *in vitro* (Chen et al., 2014).

In our previous study, it was shown that MWCNTs could inhibit the viability of C6 rat glioma cells at a concentration ranging from 50–400 μg/ml (Han et al., 2012). It was reported that 0.5-5 mg/animal of nonfunctionalized MWCNTs led to inflammation and fibrosis of lung tissue (Muller et al., 2005). Hence, a lower dose of 2.5 mg/kg, which is more clinically relevant, was used in the present study.

The MWM tests evaluated whether MWCNTs induced spatial cognitive impairments. Results indicated that exposure to MWCNTs could negatively affect the cognitive abilities of rats. In the place navigation phase, the rats of MWCNTs group required a longer time to find the platform. In addition, the constant swimming speed throughout testing of Control and MWCNTs-treated groups suggested that impaired motor

ACCEPTED MANUSCRIPT

function was not the cause of the prolonged latencies. In other words, the learning ability of the rats in this group was impaired by the MWCNTs treatment. Moreover, the quadrant dwell time and platform crossings were reduced, which indicated that the memory of rats treated by MWCNTs was affected. Re-acquisition training was used to test the re-acquisition of a new response (Walsh et al., 2011). The reversal learning is another form of cognitive flexibility. During the re-acquisition training, previously positive cues become negative and previously negative cues becomes positive (Lapiz-Bluhm et al., 2009). Our study found that MWCNTs-treated rats became worse at adapting to the change of the platform position, indicating that their capacity for cognitive flexibility was impaired compared to rats in the Control group (Fig. 3 and Fig. 4). Studies suggest that nano-materials impair performance of spatial learning and memory in the MWM test (An et al., 2012; Han et al., 2011). In addition, it was demonstrated that the water maze performance of mice could be attenuated after exposure to single-walled carbon nanotubes (SWCNTs) (Liu et al., 2014), and our results are in accordance with the above view.

The underlying mechanism of cognitive impairment was investigated in the following experiments.

Hippocampal LTP, which was recognized as an essential functional indicator of synaptic plasticity, held the key to understanding how memories were shaped (Bliss and Collingridge, 1993; Malenka and Nicoll, 1999). It was found that fEPSP slopes were significantly reduced in the MWCNTs-treated group, suggesting that LTP was impaired. This result was consistent with the data from the MWM test. Depotentiation of synaptic plasticity in the hippocampus is also regarded as a crucial mechanism for enabling the storage of new information (Morris, 2006; Qi et al., 2013). In fact, those changes were required to keep the balance between input and output of information

ACCEPTED MANUSCRIPT

for memory storage (Nicholls et al., 2008). Our data suggested that depotentiation was abnormally enhanced in the MWCNTs-treated rats. In general, the results suggested that MWCNTs induced a decrease synaptic plasticity, which could explain the lessened performance in the MWM tests. Recently, more evidence has shown that synaptic plasticity could be impeded by nanostructures (Gao et al., 2011). It is well known that synaptic plasticity in the hippocampus is associated with certain advanced functions of central nervous system, such as learning and memory. Therefore, exposure to MWCNTs may have induced impairment of hippocampal synaptic plasticity, which could contribute to the results observed in the MWM test.

N-methyl-D-aspartate (NMDA) receptors are major excitatory amino acid receptors in the central nervous system and play a pivotal role in the induction of LTP (Albensi et al., 2000). The 2B subunit (NR2B), one crucial subunit of NMDA receptors, regulates NMDA receptor activity and plays a vital role in LTP induction and learning and memory function(Clayton et al., 2002). In addition, a study reported that the NMDA receptor, including the NR2B subunit was necessary for LFS to induce depotentiation (Qi et al., 2013). Similarly, SYP is an important membrane protein of synaptic vesicles, which are closely connected with synaptic plasticity and cognitive process (Calhoun et al., 1996; Schmitt et al., 2009). We examined the expressions levels of the NR2B receptor and SYP in the hippocampus. It was found that the expression level of the NR2B subunit of the NMDA receptor was significantly reduced in MWCNTs-treated rats, and a similar trend for SYP expression was found (Fig. 6), suggesting that levels of NR2B and SYP proteins were reduced after treatment with MWCNTs. These results may uncover the underlying mechanisms for the impairments of LTP and depotentiation, as well as the cognitive deficits observed in MWM experiment.

ACCEPTED MANUSCRIPT

During fourteen consecutive treatment days, there were no differences in body weight between MWCNTs-treated rats and control rats. The most likely reason for this is that this concentration of MWCNTs has no significant effect on body weight.

The hippocampus can be divided into several regions (CA1-CA4) based on the morphology of pyramidal neurons (Eichenbaum, 2004). There is a high degree of correlation between the function of CA1 pyramidal cells and conditioned reflex, and amnesia may occur if pyramidal neurons in the CA1region are lost (Zola-Morgan et al., 1986). According to histological analyses, the nuclear shrinkage and necrotic neurons of hippocampal sections suggested that pyramidal neurons in the CA1 region were damaged after being exposed to MWCNTs, which could be confirmed by the findings obtained from our previous studies (An et al., 2012).

Many neurological disorders are related to the accumulation of autophagy in axons (Katsumata et al., 2010). It was reported that autophagy protected the brain against the development of certain types of neurodegenerative diseases (Cai and Yan, 2013; Hara et al., 2006). Therefore, induced autophagy was explored as a new area for the treatment of such diseases (García-Arencibia et al., 2010). However, the enhancement of autophagy induced by rapamycin could exacerbate the neurotoxicity of Aβ peptides (Lafay‐Chebassier et al., 2006). Moreover, the increased level of autophagy induced hippocampus-dependent synaptic impairment (Chen et al., 2013). This showed that long-lasting synaptic plasticity and memory are closely associated with mTOR-mediated protein synthesis (Costa-Mattioli et al., 2009). Autophagy led to NMDAR-dependent synaptic plasticity and brain functions through the PI3K-Akt-mTOR pathway (Shehata et al., 2012). Researchers reported that

ACCEPTED MANUSCRIPT

nanoparticles can induce autophagy in different cells *in vitro* (Luo et al., 2013; Seleverstov et al., 2006; Stern et al., 2008) and *in vivo* (Duan et al., 2014). Our study also showed that MWCNTs contributed to autophagy. We focused on the function of autophagy in MWCNTs-induced synaptic impairment in the hippocampal CA1 area.

The autophagy related proteins LC3 and Beclin-1 were measured to evaluate the levels of autophagy. It is well known that LC3 I is conjugated with phosphatidylethanolamine to form LC3 II during the process of autophagy (Klionsky et al., 2012), and autophagosomes are formed in this process. LC3 II, an active membranous protein, is localized to both the inside and the outside of autophagosomes (Mizushima et al., 2001). There is a positive correlation between the ratio of LC3 II to LC3 I and the number of autophagosomes. Therefore, detecting LC3 conversion (LC3 I to LC3 II) to measure the level of autophagy is a crucial approach (Mizushima and Yoshimori, 2007). The results of the Western blot assay showed that the LC3 II to LC3 I ratio was increased. Beclin-1 is also an important protein during the autophagy process. The autophagy level can be up-regulated by the over-expression of Beclin-1 (Kang et al., 2011). In this study, the level of Beclin-1 expression was increased in MWCNTs-treated rats. These results combined with the increased ratio of LC3 II/LC3 I suggest that autophagic activity was elevated following exposure to MWCNTs.

We used CQ, an autophagy inhibitor to further elucidate the role of autophagy in MWCNTs-induced synaptic dysfunction. CQ can inactivate autophagosomelysosome fusion, thus causing accumulation of autophagosomes in cell (Kimura et al., 2013).

ACCEPTED MANUSCRIPT

The concentration of CQ used in present study was 20mg/kg, a concentration also used by several other researchers (Maeda et al., 2013; Shintani-Ishida et al., 2014).

In our study, we found that MWCNT could cause behavioral changes in rats treated for fourteen days. Their learning and memory abilities were impaired (Fig. 2 and Fig. 3) and their synaptic plasticity was decreased (Fig. 4). Hippocampal LTP and depotentiation were considered as the electrophysiological mechanism of learning and memory. Thus, the disruption in these two indices could explain the changes observed in the rats' behavior. We also measured some biochemical indices including HE staining (Fig. 6) and Western bolt assays (Fig. 5). These biochemical indices could be used as another reason for the observed impairment in learning and memory ability.

In the present study, the consequences of exposure to MWCNTs were identified *in vivo*. Our results showed that MWCNTs could enhance the level of autophagy significantly (Fig. 5E and 5F). We also found that MWCNTs could inhibit the expression of proteins involved in synaptic plasticity (Fig. 5B and 5C) and induced neuropathological damage in the hippocampal CA1 region (Fig. 6). The spatial memory deficits including spatial learning and re-acquisition in reversal learning were significantly decreased after treatment with MWCNTs (Fig. 2, Fig. 3 and Fig. 4). More importantly, the relative indices of synaptic plasticity and cognitive deficits were considerably recovered by suppressing autophagy level with CQ. These results suggested that autophagy induced by MWCNTs might be involved in the degradation of synaptic proteins such as NR2B and SYP. This autophagy was speculated to be excessive and the decrease of autophagy level was a benefit to synaptic plasticity and

ACCEPTED MANUSCRIPT

learning and memory ability. The data clearly indicate that the increased autophagic flux plays a part in the process of MWCNTs-induced synaptic dysfunction.

5 Conclusion

In summary, our results suggest that the cognitive deficits are caused by MWCNTs via enhancing the autophagic pathway. The data suggest that the regulating autophagic process may become a new targeted therapy to relieve the damage induced by MWCNTs. To ensure the biosafety of this nanomaterial, further studies are needed to determine how autophagy regulates the dysfunction of synaptic activity.

Acknowledgments

This work was supported by grant from the National Natural Science Foundation of China (81571804, 31271074) and Tianjin Research Program of Application Foundation and Advanced Technology (14JCZDJC35000).

References

Albensi, B.C., Alasti, N. and Mueller, A.L. 2000. Long‐term potentiation in the presence of NMDA receptor antagonist arylalkylamine spider toxins. Journal of neuroscience research 62, 177-185.

An, L., Liu, S.C., Yang, Z. and Zhang, T. 2012. Cognitive impairment in rats induced by nano-CuO and its possible mechanisms. Toxicol Lett 213, 220-227.

An, L., Yang, Z. and Zhang, T. 2013. Imbalanced Synaptic Plasticity Induced Spatial Cognition

ACCEPTED MANUSCRIPT

Impairment in Male Offspring Rats Treated with Chronic Prenatal Ethanol Exposure. Alcohol Clin Exp Res 37, 763-770.

Awasthi, K.K., John, P.J., Awasthi, A. and Awasthi, K. 2013. Multi walled carbon nano tubes induced hepatotoxicity in Swiss albino mice. Micron 44, 359-364.

Belyanskaya, L., Weigel, S., Hirsch, C., Tobler, U., Krug, H.F. and Wick, P. 2009. Effects of carbon nanotubes on primary neurons and glial cells. Neurotoxicology 30, 702-711.

Bianco, A., Kostarelos, K. and Prato, M. 2005. Applications of carbon nanotubes in drug delivery. Current opinion in chemical biology 9, 674-679.

Bliss, T.V. and Collingridge, G.L. 1993. A synaptic model of memory: long-term potentiation in the hippocampus. Nature 361, 31-39.

Cai, Z. and Yan, L.-J. 2013. Rapamycin, autophagy, and Alzheimer's disease. Journal of biochemical and pharmacological research 1, 84.

Calhoun, M.E., Jucker, M., Martin, L.J., Thinakaran, G., Price, D.L. and Mouton, P.R. 1996. Comparative evaluation of synaptophysin-based methods for quantification of synapses. Journal of neurocytology 25, 821-828.

Chao, T.I., Xiang, S.H., Chen, C.S., Chin, W.C., Nelson, A.J., Wang, C.C., et al. 2009. Carbon nanotubes promote neuron differentiation from human embryonic stem cells. Biochem Bioph Res Co 384, 426-430.

Chao, T.I., Xiang, S.H., Lipstate, J.F., Wang, C.C. and Lu, J. 2010. Poly(methacrylic acid)-Grafted Carbon Nanotube Scaffolds Enhance Differentiation of hESCs into Neuronal Cells. Adv Mater 22, 3542-3547.

Chen, L., Miao, Y., Chen, L., Jin, P., Zha, Y., Chai, Y., et al. 2013. The role of elevated autophagy on the synaptic plasticity impairment caused by CdSe/ZnS quantum dots. Biomaterials 34, 10172-10181.

Chen, T., Yang, J.J., Zhang, H., Ren, G.G., Yang, Z. and Zhang, T. 2014. Multi-walled carbon nanotube inhibits CA1 glutamatergic synaptic transmission in rat's hippocampal slices. Toxicol Lett 229, 423-429.

Clayton, D.A., Mesches, M.H., Alvarez, E., Bickford, P.C. and Browning, M.D. 2002. A hippocampal NR2B deficit can mimic age-related changes in long-term potentiation and spatial learning in the Fischer 344 rat. The Journal of neuroscience 22, 3628-3637.

Costa-Mattioli, M., Sossin, W.S., Klann, E. and Sonenberg, N. 2009. Translational control of long-lasting synaptic plasticity and memory. Neuron 61, 10-26.

Das, G., Shravage, B.V. and Baehrecke, E.H. 2012. Regulation and Function of Autophagy during Cell Survival and Cell Death. Csh Perspect Biol 4.

Deng, X.Y., Wu, F., Liu, Z., Luo, M., Li, L., Ni, Q.S., et al. 2009. The splenic toxicity of water soluble multi-walled carbon nanotubes in mice. Carbon 47, 1421-1428.

Duan, J.C., Yu, Y.B., Yu, Y., Li, Y., Huang, P.L., Zhou, X.Q., et al. 2014. Silica nanoparticles enhance autophagic activity, disturb endothelial cell homeostasis and impair angiogenesis. Part Fibre Toxicol 11.

Eichenbaum, H. 2004. Hippocampus: Cognitive processes and neural representations that underlie declarative memory. Neuron 44, 109-120.

Gao, X., Yin, S., Tang, M., Chen, J., Yang, Z., Zhang, W., et al. 2011. Effects of developmental exposure to TiO2 nanoparticles on synaptic plasticity in hippocampal dentate gyrus area: an in vivo study in anesthetized rats. Biological trace element research 143, 1616-1628.

García-Arencibia, M., Hochfeld, W.E., Toh, P.P. and Rubinsztein, D.C. 2010. Autophagy, a guardian

ACCEPTED MANUSCRIPT

against neurodegeneration. Seminars in cell & developmental biology, Elsevier, pp. 691-698.

Han, D., Tian, Y., Zhang, T., Ren, G. and Yang, Z. 2011. Nano-zinc oxide damages spatial cognition capability via over-enhanced long-term potentiation in hippocampus of Wistar rats. Int J Nanomed 6, 1453-1461.

Han, G., An, L., Yang, B., Si, L. and Zhang, T. 2014. Nicotine-induced impairments of spatial cognition and long-term potentiation in adolescent male rats. Hum Exp Toxicol 33, 203-213.

Han, Y.G., Xu, J., Li, Z.G., Ren, G.G. and Yang, Z. 2012. In vitro toxicity of multi-walled carbon nanotubes in C6 rat glioma cells. Neurotoxicology 33, 1128-1134.

Hara, T., Nakamura, K., Matsui, M., Yamamoto, A., Nakahara, Y., Suzuki-Migishima, R., et al. 2006. Suppression of basal autophagy in neural cells causes neurodegenerative disease in mice. Nature 441, 885-889.

Kang, R., Zeh, H., Lotze, M. and Tang, D. 2011. The Beclin 1 network regulates autophagy and apoptosis. Cell Death & Differentiation 18, 571-580.

Katsumata, K., Nishiyama, J., Inoue, T., Mizushima, N., Takeda, J. and Yuzaki, M. 2010. Dynein-and activity-dependent retrograde transport of autophagosomes in neuronal axons. Autophagy 6, 378-385.

Kaushik, S., Rodriguez-Navarro, J.A., Arias, E., Kiffin, R., Sahu, S., Schwartz, G.J., et al. 2011. Autophagy in Hypothalamic AgRP Neurons Regulates Food Intake and Energy Balance. Cell Metab 14, 173-183.

Keefer, E.W., Botterman, B.R., Romero, M.I., Rossi, A.F. and Gross, G.W. 2008. Carbon nanotube coating improves neuronal recordings. Nat Nanotechnol 3, 434-439.

Kenzaoui, B.H., Bernasconi, C.C., Guney-Ayra, S. and Juillerat-Jeanneret, L. 2012. Induction of oxidative stress, lysosome activation and autophagy by nanoparticles in human brain-derived endothelial cells. Biochem J 441, 813-821.

Kimura, T., Takabatake, Y., Takahashi, A. and Isaka, Y. 2013. Chloroquine in cancer therapy: a double-edged sword of autophagy. Cancer Res 73, 3-7.

Klionsky, D.J., Abdalla, F.C., Abeliovich, H., Abraham, R.T., Acevedo-Arozena, A., Adeli, K., et al. 2012. Guidelines for the use and interpretation of assays for monitoring autophagy. Autophagy 8, 445-544.

Klionsky, D.J., Cuervo, A.M. and Seglen, P.O. 2007. Methods for monitoring autophagy from yeast to human. Autophagy 3, 181-206.

Kroemer, G., Marino, G. and Levine, B. 2010. Autophagy and the Integrated Stress Response. Molecular cell 40, 280-293.

Lafay‐Chebassier, C., Pérault‐Pochat, M.C., Page, G., Bilan, A.R., Damjanac, M., Pain, S., et al. 2006. The immunosuppressant rapamycin exacerbates neurotoxicity of Aβ peptide. Journal of neuroscience research 84, 1323-1334.

Lapiz-Bluhm, M.D.S., Soto-Piña, A.E., Hensler, J.G. and Morilak, D.A. 2009. Chronic intermittent cold stress and serotonin depletion induce deficits of reversal learning in an attentional set-shifting test in rats. Psychopharmacology 202, 329-341.

Li, J.G., Li, W.X., Xu, J.Y., Cai, X.Q., Liu, R.L., Li, Y.J., et al. 2007. Comparative study of pathological lesions induced by multiwalled carbon nanotubes in lungs of mice by intratracheal instillation and inhalation. Environ Toxicol 22, 415-421.

Liu, X.D., Zhang, Y.C., Li, J.Q., Wang, D., Wu, Y., Li, Y., et al. 2014. Cognitive deficits and decreased locomotor activity induced by single-walled carbon nanotubes and neuroprotective effects of ascorbic acid. Int J Nanomed 9, 823-839.

ACCEPTED MANUSCRIPT

Luo, Y.H., Wu, S.B., Wei, Y.H., Chen, Y.C., Tsai, M.H., Ho, C.C., et al. 2013. Cadmium-Based Quantum Dot Induced Autophagy Formation for Cell Survival via Oxidative Stress. Chem Res Toxicol 26, 662-673.

Ma, X.W., Wu, Y.Y., Jin, S.B., Tian, Y., Zhang, X.N., Zhao, Y.L., et al. 2011. Gold Nanoparticles Induce Autophagosome Accumulation through Size-Dependent Nanoparticle Uptake and Lysosome Impairment. Acs Nano 5, 8629-8639.

Maeda, H., Nagai, H., Takemura, G., Shintani-Ishida, K., Komatsu, M., Ogura, S., et al. 2013. Intermittent-hypoxia induced autophagy attenuates contractile dysfunction and myocardial injury in rat heart. Bba-Mol Basis Dis 1832, 1159-1166.

Malenka, R.C. and Nicoll, R.A. 1999. Long-term potentiation--a decade of progress? Science 285, 1870-1874.

Mizushima, N. 2007. Autophagy: process and function. Gene Dev 21, 2861-2873.

Mizushima, N. and Komatsu, M. 2011. Autophagy: Renovation of Cells and Tissues. Cell 147, 728-741.

Mizushima, N., Yamamoto, A., Hatano, M., Kobayashi, Y., Kabeya, Y., Suzuki, K., et al. 2001. Dissection of autophagosome formation using Apg5-deficient mouse embryonic stem cells. Journal of Cell Biology 152, 657-667.

Mizushima, N. and Yoshimori, T. 2007. How to interpret LC3 immunoblotting. Autophagy 3, 542-545.

Mizushima, N., Yoshimori, T. and Levine, B. 2010. Methods in Mammalian Autophagy Research. Cell 140, 313-326.

Morris, R.G.M. 2006. Elements of a neurobiological theory of hippocampal function: the role of synaptic plasticity, synaptic tagging and schemas. Eur J Neurosci 23, 2829-2846.

Muller, J., Huaux, F., Moreau, N., Misson, P., Heilier, J.F., Delos, M., et al. 2005. Respiratory toxicity of multi-wall carbon nanotubes. Toxicol Appl Pharm 207, 221-231.

Nakashima, N. and Fujigaya, T. 2007. Fundamentals and applications of soluble carbon nanotubes. Chem Lett 36, 692-697.

Nicholls, R.E., Alarcon, J.M., Malleret, G., Carroll, R.C., Grody, M., Vronskaya, S., et al. 2008. Transgenic mice lacking NMDAR-dependent LTD exhibit deficits in behavioral flexibility. Neuron 58, 104-117.

Poels, J., Spasic, M.R., Callaerts, P. and Norga, K.K. 2012. An appetite for destruction From self-eating to cell cannibalism as a neuronal survival strategy. Autophagy 8, 1401-1403.

Qi, Y.J., Hu, N.W. and Rowan, M.J. 2013. Switching off LTP: mGlu and NMDA Receptor-Dependent Novelty Exploration-Induced Depotentiation in the Rat Hippocampus. Cerebral Cortex 23, 932-939.

Ren, J.F., Shen, S., Wang, D.G., Xi, Z.J., Guo, L.R., Pang, Z.Q., et al. 2012. The targeted delivery of anticancer drugs to brain glioma by PEGylated oxidized multi-walled carbon nanotubes modified with angiopep-2. Biomaterials 33, 3324-3333.

Sanchez-Varo, R., Trujillo-Estrada, L., Sanchez-Mejias, E., Torres, M., Baglietto-Vargas, D., Moreno-Gonzalez, I., et al. 2012. Abnormal accumulation of autophagic vesicles correlates with axonal and synaptic pathology in young Alzheimer's mice hippocampus. Acta Neuropathol 123, 53-70.

Schmitt, U., Tanimoto, N., Seeliger, M., Schaeffel, F. and Leube, R. 2009. Detection of behavioral alterations and learning deficits in mice lacking synaptophysin. Neuroscience 162, 234-243.

Seleverstov, O., Zabirnyk, O., Zscharnack, M., Bulavina, L., Nowicki, M., Heinrich, J.M., et al. 2006. Quantum dots for human mesenchymal stem cells labeling. A size-dependent autophagy activation. Nano Lett 6, 2826-2832.

ACCEPTED MANUSCRIPT

Shehata, M., Matsumura, H., Okubo-Suzuki, R., Ohkawa, N. and Inokuchi, K. 2012. Neuronal stimulation induces autophagy in hippocampal neurons that is involved in AMPA receptor degradation after chemical long-term depression. The Journal of Neuroscience 32, 10413-10422.

Shen, S., Kepp, O. and Kroemer, G. 2012. The end of autophagic cell death? Autophagy 8, 1-3.

Shintani-Ishida, K., Saka, K., Yamaguchi, K., Hayashida, M., Nagai, H., Takemura, G., et al. 2014. MDMA induces cardiac contractile dysfunction through autophagy upregulation and lysosome destabilization in rats. Bba-Mol Basis Dis 1842, 691-700.

Sorkin, R., Gabay, T., Blinder, P., Baranes, D., Ben-Jacob, E. and Hanein, Y. 2006. Compact self-wiring in cultured neural networks. Journal of neural engineering 3, 95-101.

Stern, S.T., Zolnik, B.S., McLeland, C.B., Clogston, J., Zheng, J.W. and McNeil, S.E. 2008. Induction of autophagy in porcine kidney cells by quantum dots: A common cellular response to nanomaterials? Toxicol Sci 106, 140-152.

Walsh, C.M., Booth, V. and Poe, G.R. 2011. Spatial and reversal learning in the Morris water maze are largely resistant to six hours of REM sleep deprivation following training. Learn Memory 18, 422-434.

Wang, C.Y., Zhang, Y.Y., Wang, C.M. and Tan, V.B.C. 2007. Buckling of carbon nanotubes: A literature survey;. Journal of nanoscience and nanotechnology 7, 4221-4247.

Yang, D., Yang, F., Hu, J., Long, J., Wang, C., Fu, D., et al. 2009. Hydrophilic multi-walled carbon nanotubes decorated with magnetite nanoparticles as lymphatic targeted drug delivery vehicles. Chem Commun, 4447-4449.

Yang, Z., Zhang, Y., Yang, Y., Sun, L., Han, D., Li, H., et al. 2010a. Pharmacological and toxicological target organelles and safe use of single-walled carbon nanotubes as drug carriers in treating Alzheimer disease. Nanomedicine: Nanotechnology, Biology and Medicine 6, 427-441.

Yang, Z., Zhang, Y.G., Yang, Y.L.A., Sun, L., Han, D., Li, H., et al. 2010b. Pharmacological and toxicological target organelles and safe use of single-walled carbon nanotubes as drug carriers in treating Alzheimer disease. Nanomed-Nanotechnol 6, 427-441.

Zhang, Y., Ali, S.F., Dervishi, E., Xu, Y., Li, Z., Casciano, D., et al. 2010. Cytotoxicity effects of graphene and single-wall carbon nanotubes in neural phaeochromocytoma-derived PC12 cells. Acs Nano 4, 3181-3186.

Zola-Morgan, S., Squire, L.R. and Amaral, D.G. 1986. Human amnesia and the medial temporal region: enduring memory impairment following a bilateral lesion limited to field CA1 of the hippocampus. J Neurosci 6, 2950-2967.

Figure captions

Fig. 1. The effects of treatment with MWCNTs and CQ on rat body weight. Data represent mean ± SEM. n = 8 per group.

ACCEPTED MANUSCRIPT

Fig. 2. The results of MWM experiments in initial training stage. **A**: Mean escape latency was calculated for 5 days in place navigation phase. **B**: Mean swimming speed in place navigation phase. **C**: Mean number of platform area crossings in spatial probe phase. **D**: Mean percentage of time spent in target quadrant in spatial probe phase. Data are expressed as mean ± SEM. $^{*}P<0.05$, $^{**}P<0.01$, $^{***}P<0.01$ comparison between control group versus MWCNTs-treated group; $^{\#}P<0.05$, $^{\#\#}P<0.01$ comparison between MWCNTs-treated and MWCNTs+CQ group; n = 8 per group.

Fig. 3. The results of MWM experiments in re-acquisition training stage. **A**: Mean escape latency was calculated for 3 days in place navigation phase. **B**: Mean swimming speed in place navigation phase. **C**: Mean number of platform crossings in spatial probe phase. **D**: Mean percentage of time spent in target quadrant in spatial probe phase. Data represent mean ± SEM. $^{**}P<0.01$, $^{***}P<0.001$comparison between control group and MWCNTs-treated group; $^{\#}P<0.05$ comparison between MWCNTs-treated and MWCNTs+CQ group; n = 8 per group.

Fig. 4. The effects of MWCNTs exposure on long-term potentiation (LTP) and depotentiation. **A**: The first 30 minutes of evoked responses were normalized and used as the baseline responses of LTP. **B**: Magnitude of LTP was determined as responses between 40 and 60 minutes after a theta burst stimulation (TBS). **C**: Magnitude of depotentiation was determined as the responses between 30 and 60 minutes after low-frequency stimulation (LFS). **D**: The last 30 minutes of evoked responses during LTP were normalized and used as the baseline responses of depotentiation. Data are expressed as mean ± SEM. $^{***}P<0.001$ comparison between

ACCEPTED MANUSCRIPT

control group versus MWCNTs-treated group； $^{###}P<0.001$ comparison between MWCNTs-treated and MWCNTs+CQ group; n = 8 per group.

Fig. 5. Western blot assays were carried out to analyze the expression of NR2B, PSD-95, LC3 and Beclin-1 in the hippocampus after exposure to MWCNTs. 30 μg of proteins were separated on a 10% SDS−PAGE gel and were subjected to a Western blot assay. **A**: The proteins were further probed with NR2B, SYP antibodies and anti-β-actin antibodies (one representative Western blot assay is shown; n = 4). **B**: Bands density of NR2B and SYP were measured. **C**: 30μg of proteins were separated on a 13%SDS−PAGE gel and were subjected to Western blotting assay. The proteins were further probed with LC3, Beclin1 antibodies and anti-β-actin antibodies (one representative Western blot assay is shown; n = 4). **D**: Bands density LC3-II/LC3-I and Beclin-1 were measured. Data are presented as mean ± SEM. $^{***}P<0.001$, comparison between Con group and MWCNTs-treated group; $^{#}P<0.05$, $^{##}P<0.01$, $^{###}P<0.001$ comparison between MWCNTs-treated and MWCNTs+CQ group.

Fig. 6. The results of morphology in hippocampal neurons revealed by HE staining (×40). **A**: The hippocampal neurons in control group. **B**: The hippocampal neurons in MWCNT-treated group. **C**: The hippocampal neurons in MWCNT+CQ group.

ACCEPTED MANUSCRIPT

Fig. 1

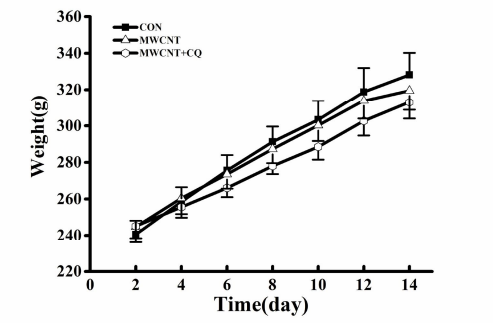

Fig. 1

Fig. 2

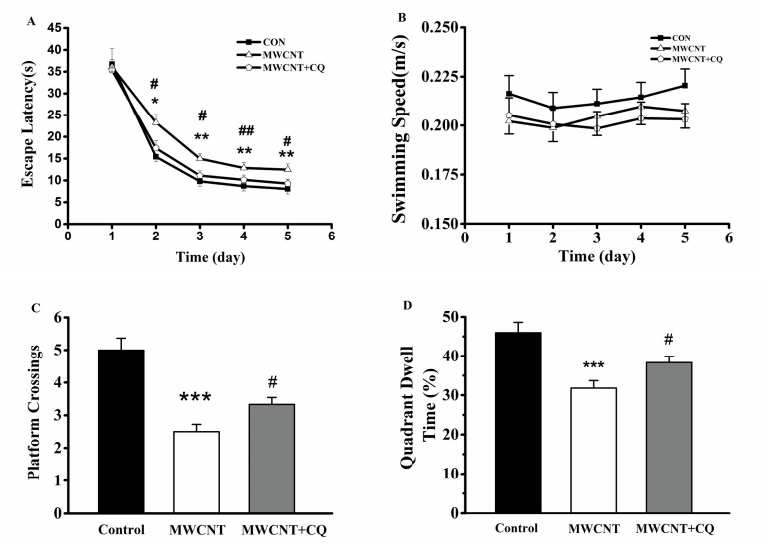

Fig. 2

ACCEPTED MANUSCRIPT

Fig. 3

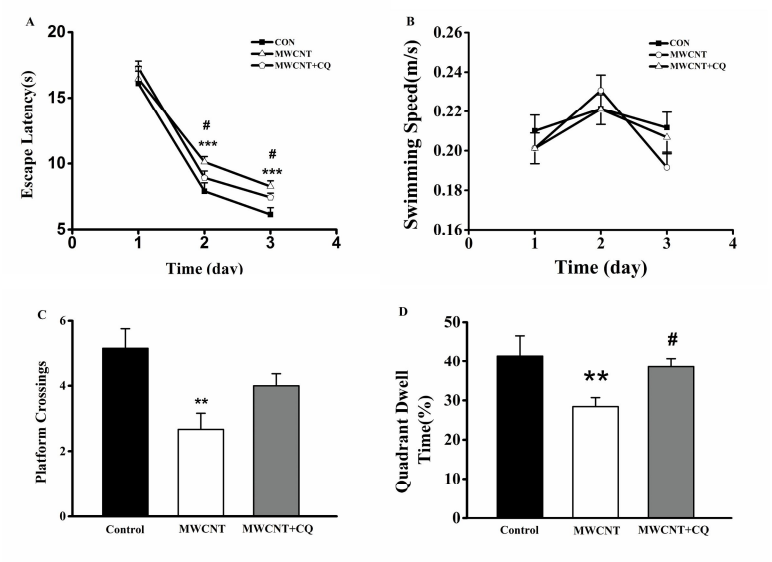

Fig. 3

Fig. 4

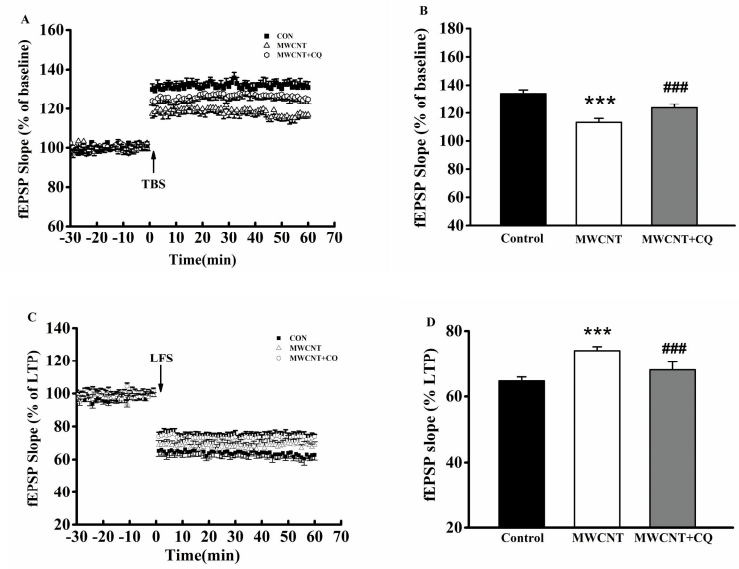

Fig. 4

ACCEPTED MANUSCRIPT

Fig. 5

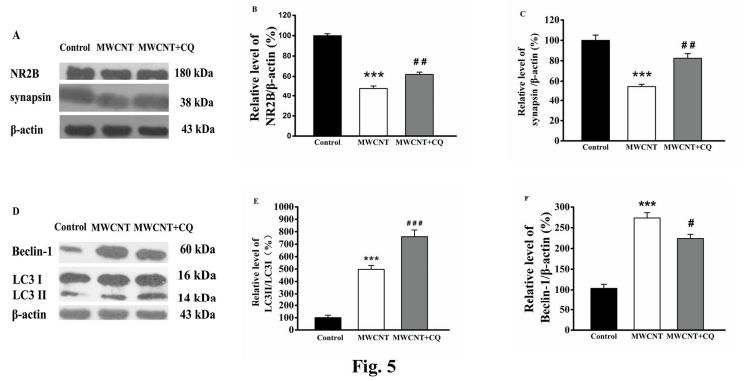

Fig. 5

Fig. 6

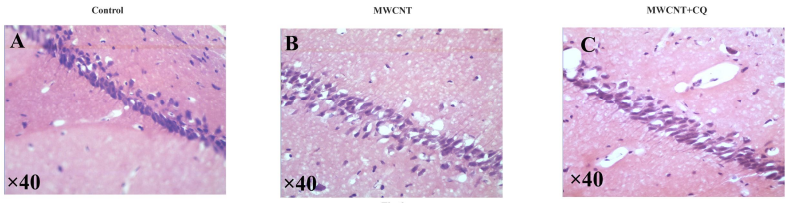

Fig.6